25th ABCM International Congress of Mechanical Engineering
October 20-25, 2019, Uberlândia, MG, Brazil

COB-2019-0507
INFLUENCE OF DIFFERENT RANDOM PROCESSES IN THE RESPONSE OF A NONLINEAR PIEZOMAGNETOELASTIC GENERATOR

Filipe Eduard Leite Ossege
Aline Souza de Paula
Tiago Leite Pereira
Adriano Todorovic Fabro
Department of Mechanical Engineering, Universidade de Brasília, 70.910-900, Brasília, DF
eduard.ossege@gmail.com - alinedepaula@unb.br - tiagolei.tl@gmail.br - fabro@unb.br

Abstract. *Piezoelectric energy harvesters devices can be a good alternative to support low power devices in order to achieve self powered sensors and actuators. In this work, a nonlinear piezomagnetoelastic generator is investigated. The system consists of a ferromagnetic cantilever beam with two permanent magnets in a bistable configuration. The device captures the energy from the environment vibration using piezoelectric material, once this material naturally converts mechanical energy into electrical energy. As in the investigation performed by previous authors, this work presents an analysis of the harvested energy when the system is subjected by a combination of harmonic and random excitation. The present work, different from the cited reference, treats different Power Spectrum Density (PSD) functions.*

Keywords: *piezoelectric material, energy harvesting, random excitation, nonlinearities*

1. INTRODUCTION

Renewable energy solutions are necessary nowadays since most of world's energy use are provenient from fossil fuels, which brings negative impacts, being the dominant source of local air pollution and emitter of carbon dioxide and other greenhouse gases. Piezoelectric energy harvesters devices based on mechanical vibration takes almost no damage to the environment. These harvesters can be a good alternative to support low power devices in order to achieve self powered sensors and actuators.

Linear piezoelectric energy harvesters are quite sensitive to frequency variations, presenting good performance only at resonance frequencies, whereas non linear systems can be more efficient within a range of frequency (De Paula *et al.*, 2015; Erturk *et al.*, 2009). Once nature provides random vibration in almost every ecosystem, consider a portion of the external excitation random consists in a realistic assumption.

A variety of cases has already been analyzed in the context of piezoelectric energy harvesters. Lallart *et al.* (2010) showed the sensibility of linear systems and how to maintain them in the resonance frequency with self-tuned system. Litak *et al.* (2016) presented a piezoelectric energy harvester with regular and chaotic vibration. Feenstra *et al.* (2008) covered an harvesting system based on a packback that generates electrical energy from the forces between the wearer and the pack. Rome *et al.* (2005) used a suspended load backpack to provide electricity through normal walking. Sohn *et al.* (2005) investigated the use of piezoelectric material for micro-electro-mechanical systems (MEMS) which benefit from fluctuating blood pressure by means of the finite element method (FEM). De Paula *et al.* (2015) provided a study of piezo-magnetoelastic structure subjected to random vibrations and analysed linear, nonlinear monostable and nonlinear bistable cases. It is shown that nonlinearity is used to spread the energy through a broadband frequency. Pereira *et al.* (2019) studied the efficiency of the same structure under three types of excitation: pure harmonic, pure random and harmonic and random combination. For the random excitation, a Gaussian white noise is analyzed.

In the present work, the same piezomagnetoelastic structure considered by Pereira *et al.* (2019); De Paula *et al.* (2015) and other authors is studied. The device captures the energy from the environment vibration using piezoelectric material, once this material naturally converts mechanical energy into electrical energy. The system consists of a ferromagnetic cantilever beam with two permanent magnets in a bistable configuration.

As in the investigation performed by Pereira *et al.* (2019), this work presents an analysis of the harvested energy when the system is subjected by a combination of harmonic and random excitation. The present work, different from the cited reference, treats different Power Spectrum Density (PSD) functions for the random excitation. These PSD functions physically sound and better represent natural phenomena than Gaussian white noise.

2. PIEZOMAGNETOELASTIC STRUCTURE AND ENERGY HARVESTED EVALUATION

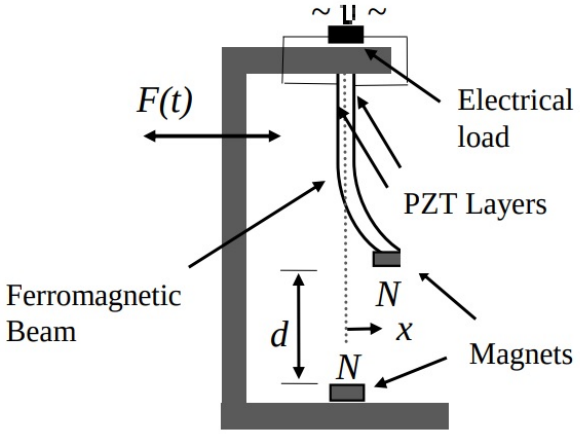

Figure 1: Schematic representation of the piezomagnetoelastic structure.
(De Paula *et al.*, 2015)

Figure 1 presents a schematic representation of the structure that consists of a ferromagnetic cantilever beam with two permanent magnets, one located at the free end of the beam and the other at a vertical distance d from free end. The piezoelectric layers are connected to an electrical circuit that, for the sake of simplicity, can be represented by a resistor. Base excitation is represented by a combination of random and harmonic excitations.

By assuming a linear electromechanical piezoelectric coupling, system behavior can be described by the following equations:

$$\ddot{u} + 2\xi\dot{u} - \frac{1}{2}u(1-u^2) - \chi\nu = F(t) \tag{1}$$

$$\dot{\nu} + \lambda\nu + \kappa\dot{u} = 0 \tag{2}$$

where u is the dimensionless horizontal displacement of the tip of the beam, $\dot{u}$ is the dimensionless speed of this displacement, ν is the dimensionless electric tension across the load resistance, ξ is the dimensionless mechanical damping ratio, χ is the dimensionless piezoelectric coupling term in the mechanical equation, κ is the dimensionless piezoelectric coupling term in the electrical circuit equation, λ is the dimensionless time constant and $F(t)$ is the dimensionless excitation due to base movement.

The parameters are considered exactly the same as in Erturk *et al.* (2009): $\xi = 0.01$, $\chi = 0.05$, $\kappa = 0.5$ and $\lambda = 0.05$. By considering these values, system has three equilibrium points: two stable spiral points at $(u, \dot{u}, \nu) = (\pm 1, 0, 0)$ and one unstable saddle point at $(u, \dot{u}, \nu) = (0, 0, 0)$.

The external excitation is described by a combination of harmonic and random forces, as follows:

$$F(t) = F_0 \cos(\Omega t) + p(\bar{u}, \sigma) \tag{3}$$

where F_0 is the dimensionless excitation amplitude, Ω is the dimensionless angular velocity of the excitation, t is the dimensionless time and p represents a probability distribution with mean value $\bar{u}$ and standard deviation σ.

The harvested energy is evaluated based on Power Spectral Density (PSD), as proposed by Pereira *et al.* (2019), defined as:

$$PSD(\omega) = \frac{\left|\hat{x}(\omega)\right|^2}{T} \tag{4}$$

where T is the total dimensionless time of analysis, ω is the dimensionless frequency of the signal and $\hat{x}(\omega)$ is the Fourier Transform of the signal $x(t)$. Note that $\hat{x}(\omega)$ is defined as

$$\hat{x}(\omega) = \int_{-\infty}^{\infty} e^{-2\pi i\omega t} x(t) dt \tag{5}$$

where $i = \sqrt{-1}$.

Also, note that $x(t)$ can be determined by the Inverse Fourier Transform:

$$x(t) = \int_{-\infty}^{\infty} e^{2\pi i \omega t} \hat{x}(\omega) d\omega \tag{6}$$

A Fast Fourier Transform (FFT) algorithm and Hanning windowing (Newland, 1980) are used to calculate Eq. (4), Eq. (5) and Eq. (6).

Furthermore, the power of the signal itself is calculated as the area under the curve of PSD:

$$P = \int_{0}^{\omega_u} PSD(\omega) d\omega \tag{7}$$

where $[0, \omega_u]$ is the range of frequency of interest and P is the dimensionless power of the signal.

One way to verify the efficiency of the system is to compare the excitation (input) and the voltage (output) generated. Thus, a ratio r is defined:

$$r = \frac{P_\nu}{P_F} = \frac{\int_0^{\omega_u} PSD_\nu(\omega) d\omega}{\int_0^{\omega_u} PSD_F(\omega) d\omega} \tag{8}$$

where P_F is the power of the signal $x(t) = F(t)$ and P_ν the power of $x(t) = \nu(t)$. PSD_F and PSD_ν are their respective Power Spectral Densities.

Since all variables used in this article are dimensionless, the value of r in Eq. (8) can be greater than 1.

For the case of pure random excitation, the PSD_F is first defined and then the excitation $F(t)$ is calculated by Eq. (6) and Eq. (4). Evaluating $F(t)$ at Eq. (1) and Eq. (2), the rest of the variables are calculated.

The formula for the PSD_F used in this article for pure random excitation $F(t) = p(\bar{u}, \sigma)$ is defined as follows

$$PSD_F(\omega, n, \sigma, v) = \frac{\sigma^2}{v^n + (2\pi\omega)^n} \tag{9}$$

where σ is the standard deviation, n is the degree of the PSD and v is a filter parameter. A similar PSD is analyzed by Alkmim *et al.* (2016), a first order filter, in which $n = 1$. In this work, an n order filter is used. The considered PSD physically sounds.

3. RESULTS

3.1 Harmonic Excitation

At first pure harmonic excitation is of concern. Figure 2 presents time response, phase space together with Poincaré section and PSD_F and PSD_ν in steady state when the excitation is given by $F(t) = F_0 \cos(\Omega t)$, with $\Omega = 0.8$ and $F_0 = 0.083$. Two situations are of concern, being one periodic response, obtained with $(u_0, \dot{u}_0, \nu_0) = (1, 1, 0)$, and the other a chaotic behavior, obtained with $(u_0, \dot{u}_0, \nu_0) = (1, 0, 0)$. u_0, $\dot{u}_0$ and ν_0 are the initial conditions of the system.

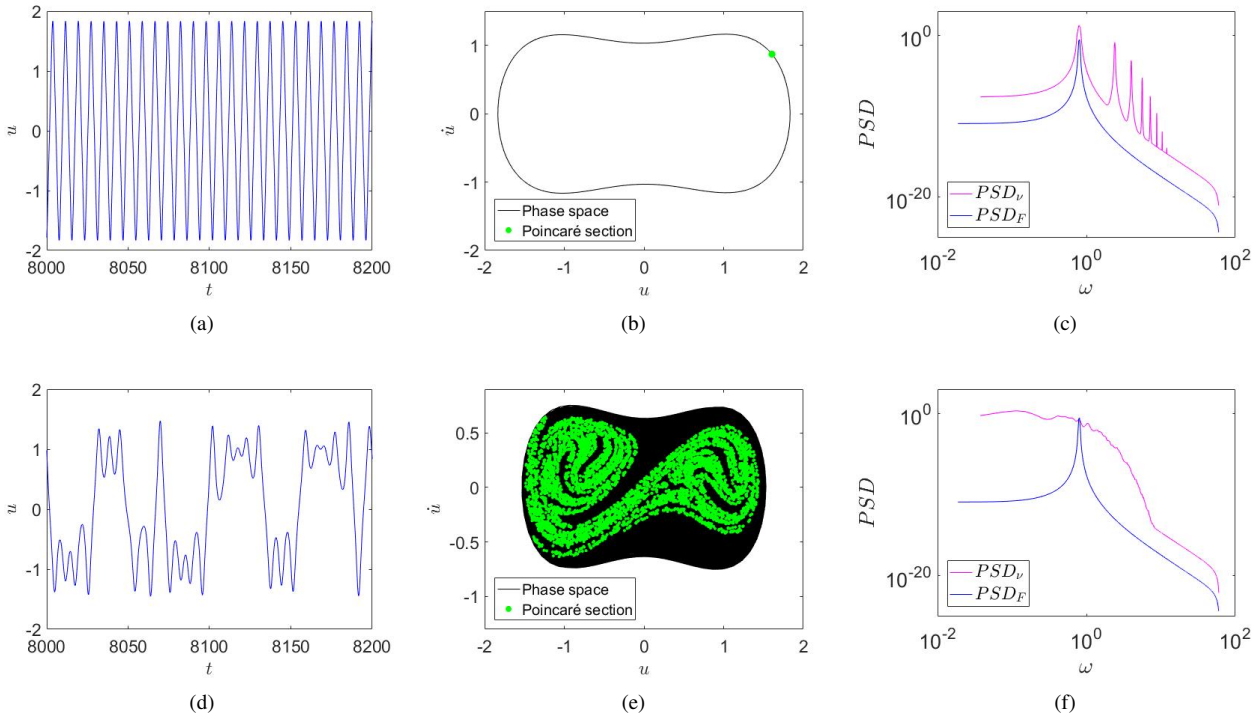

Figure 2: System response in steady state with pure harmonic excitation: displacement (a,d), phase space together with Poincaré section (b,e), PSD of voltage and PSD of displacement (c,f) with initial conditions: (a)-(c) $(u_0, \dot{u}_0, \nu_0) = (1, 1, 0)$; (d)-(f) $(u_0, \dot{u}_0, \nu_0) = (1, 0, 0)$.

Table 1: Results for either periodic or chaotic behaviour of the system.

Behaviour	r	P_ν
Periodic$^{(1)}$	102.242	40.924
Chaotic$^{(2)}$	43.693	17.489

$^{(1)}$ $(u_0, \dot{u}_0, \nu_0) = (1, 1, 0)$
$^{(2)}$ $(u_0, \dot{u}_0, \nu_0) = (1, 0, 0)$

Table 1 shows the values of r and P_ν for each case. The power of the excitation remains constant and equals to $P_F = 0.400$ for both cases. Comparing values of r and P_ν, the presented periodic response present a better performance when compared to the chaotic situation.

3.2 Random Excitation

At this point, pure random excitation is considered. Figure 3 presents time response, phase space and PSD_F and PSD_ν in steady state for $(u_0, \dot{u}_0, \nu_0) = (1, 0, 0)$, a stable equilibrium point. The excitation is given by $F(t) = p(\bar{u}, \sigma) = N(\bar{u}, \sigma)$, where N is a Gaussian white noise, as considered by Pereira *et al.* (2019). The mean value is fixed at $\bar{u} = 0$ and different values of standard deviation are considered: Figure 3a-3c presents the results for $\sigma = 0.1$, where $r = 0.033$ is obtained; Fig. 3d-3f presents results for $\sigma = 0.42$, with $r = 0.079$; while Fig. 3g-3i presents results for $\sigma = 1$, where $r = 0.133$ is obtained. For the 3 values of σ considered, higher values are associated with better performance of the generator (higher value of r).

Table 2: Results for each standart deviation of the system with normally distributed excitation.

σ	r	P_ν	P_F
0.1	0.033	0.038	1.161
0.42	0.079	1.625	20.472
1	0.133	15.412	116.054

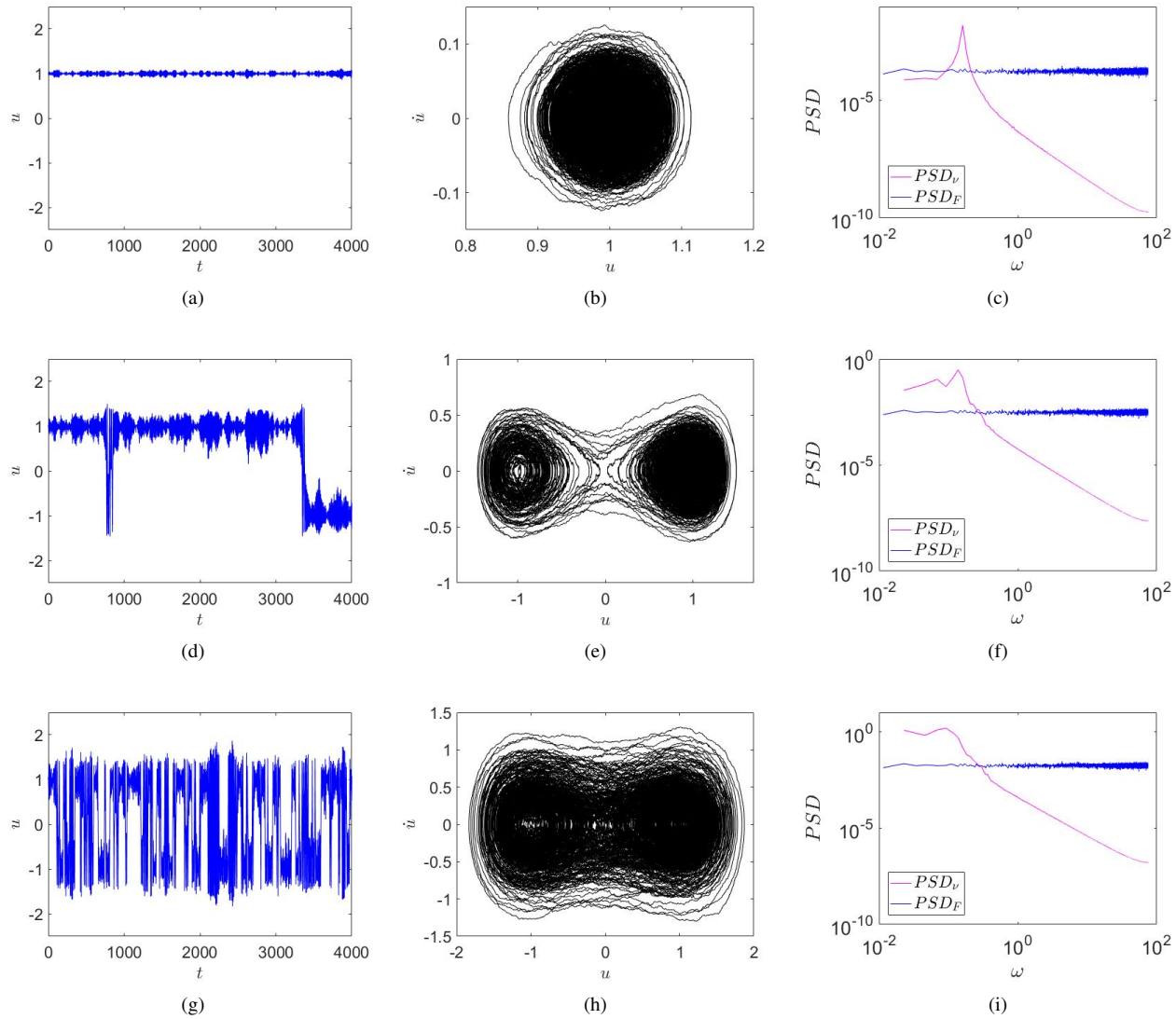

Figure 3: System response in steady state with pure random excitation: displacement (a,d,g), phase space (b,e,h), PSD of voltage and PSD of displacement (c,f,i) with initial value $(u_0, \dot{u}_0, \nu_0) = (1, 0, 0)$, mean value $\bar{u} = 0$ and standard deviation: (a)-(c) $\sigma = 0.1$; (d)-(f) $\sigma = 0.42$; (g)-(i) $\sigma = 1$.

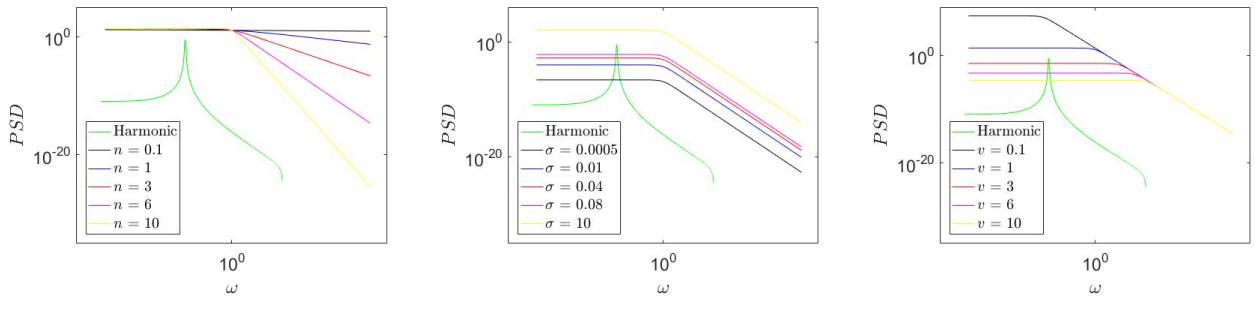

Figure 4: PSD of an harmonic signal (green) and PSDs with $\sigma = 5$, $n = 6$ and $v = 1$ fixed. Each graph shows the variation of a variable: a) n; b) σ; c) v.

At this point, different random excitation are considered by varying values of n, σ and v. Figure 4 shows how each variable changes the format of the PSD, defined by Eq. (9). Figure 4b shows how the standart deviation modify the PSD. Note that the increase of σ cause an increase of the area under the curve of the $PSD(\omega)$ function. Thus, the power

available to the system is higher. Figures 4a and 4c show the influence of n and v, respectively. Note that, different from σ, higher values of n and v decrease the area under the curve. Thus, the power available to the system is lower. The PSD of the harmonic excitation (green curve) is also presented in Figure 4.

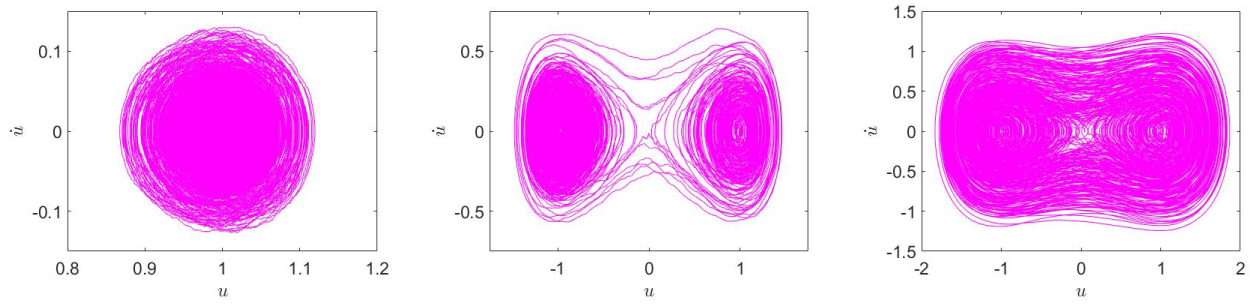

(a) (b) (c)

Figure 5: Phase space for $\sigma = 0.08$, $v = 1$, with initial value $(u_0, \dot{u}_0, \nu_0) = (1, 0, 0)$ and different degrees: a) $n = 0.1$; b) $n = 1$; c) $n = 2$.

Figure 5 shows system response in phase space with $\sigma = 0.08$, $v = 1$ and different values of n. Note that the same tendency observed in Fig. 3 is obtained. In Fig. 5a system oscillates around only one stable equilibrium point, which leads to small value of output power, as presented in Fig. 6. When system starts to oscillate around both stable equilibrium point, as presented in Fig. 5b, the output power increases. Figure 5c presents the best situation for energy harvesting purpose, when both stable equilibrium points are visited with high level of transition between equilibrium points. These kind of behaviors are representative for all analyzed cases, where situations related to Fig. 5c are of interest.

Since the excitation is random, the response, including output power and efficiency, varies in each time the algorithm runs. Thus, for each set of parameter, the algorithm runs 10 times and the mean values of desired variables are calculated, as presented in Fig. 6, that presents efficiency and power input and output for each analyzed case. Note that highest values of output power are associated with the behavior presented in Fig. 5c.

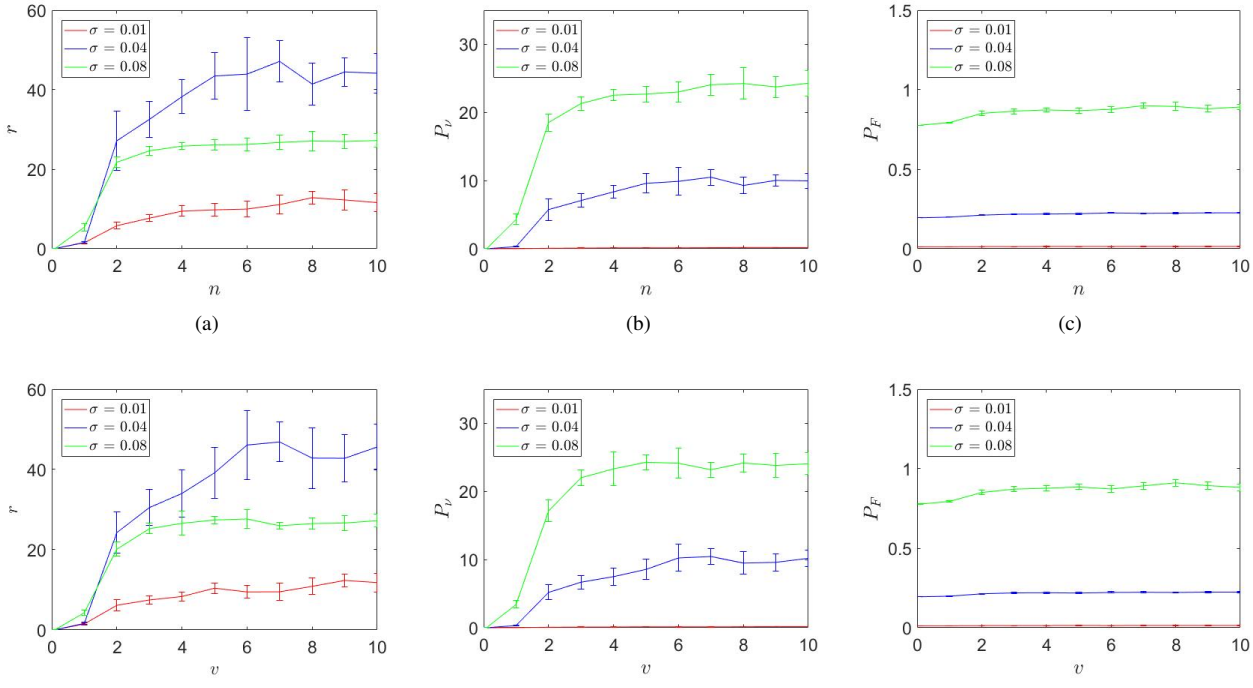

(a) (b) (c)

(d) (e) (f)

Figure 6: System behaviour for random excitation: values of r, a) and d); P_ν, b) and e); and P_f, c) and f), with initial value $(u_0, \dot{u}_0, \nu_0) = (1, 0, 0)$ as a)-c) n varies; d)-c) v varies.

Values of σ higher that 0.08 are not considered as it leads to extremely large amplitude oscillations of the system and do not represent real situations.

Note that for $\sigma = 0.04$ the system presents the highest efficiency. In contrast, $\sigma = 0.08$ are related to the highest values of output power (P_ν). The best case scenario chosen is the one with the highest voltage power.

Note that n and v present similar effects in the values of P_ν. Higher values than $n = 2$ and $v = 3$ do not change the power output significantly.

3.3 Combined Excitation

At last, the combined excitation is of concern, where $F(t) = F_0 \cos(\Omega t) + p(\bar{u}, \sigma)$. Then, the combined excitation $F(t)$ is used to computed PSD_F using Eq. (5) followed by Eq. (4). Based on previous results, it is considered $\sigma = 0.08$ and $v = 3$ and the goal is to obtain the maximum value of P_ν. The analysis begins from the two attractors considered in the case of pure harmonic excitation (with $\Omega = 0.8$ and $F_0 = 0.083$), one periodic and one chaotic. From these two behavior, random excitation is added and values of n in increased.

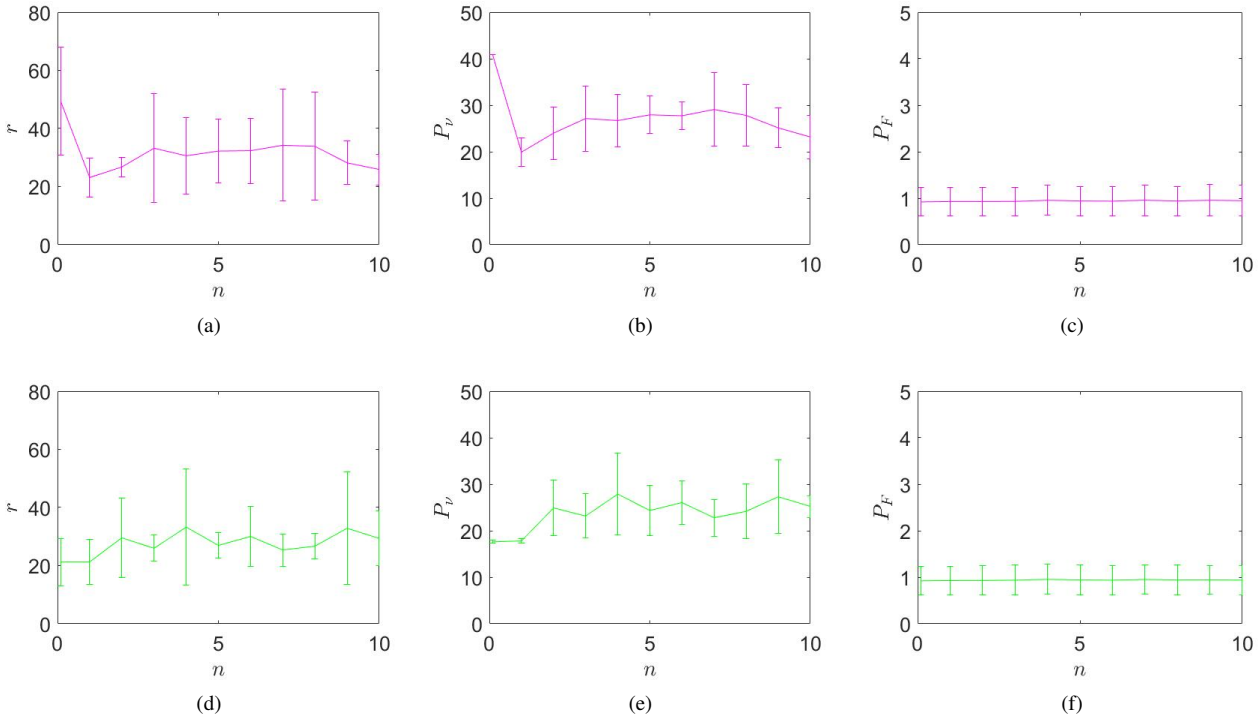

Figure 7: System behaviour for combined excitation: values of r, a) and d); P_ν, b) and e); and P_f, c) and f), for $\sigma = 0.08$ and $v = 3$ with: a)-c) Periodic behaviour - $(u_0, \dot{u}_0, \nu_0) = (1, 1, 0)$; d)-f) Chaotic behaviour - $(u_0, \dot{u}_0, \nu_0) = (1, 0, 0)$.

From Fig. 7 one can conclude that the best case scenario is the periodic behaviour with degree $n = 0.1$. Note that, from Eq. (9), for small n, the PSD_F function approaches to $\sigma^2/2$. This returns a Gaussian Distribution for the PSD. In general, note that the addition of random excitation in the periodic response decreases power output, while when added in the chaotic response promotes an increase of power output. Moreover, for values of n equal or bigger than 2, power output is similar in both situation, as presented in Figs. 7b and 7e. This result indicated that the same kind of behavior occurs, possibly there is an intermittency between the two attractor, causing the appearance of a new regime of mixed-mode stochastic oscillations, as reported by Bashkirtseva *et al.* (2018)

4. CONCLUSION

From the investigation with pure harmonic excitation, this paper presents consistent results when compared to the literature. In the analysis of pure random excitation, better results in the context of energy harvesting are obtained when system oscillates between the two stable equilibrium points and appropriate values of n, σ and v are presented. Although n and v present different PSD curves, their influence on power output is similar. From combined excitation analysis, results show that the addition of random excitation in the periodic response decreases power output, while its addition in the chaotic response promotes an increase of power output. Possibly the addition of random excitation leads to an intermittency between the two attractor identified in the case of pure harmonic excitation.

5. ACKNOWLEDGEMENTS

The authors would like to acknowledge the support of the Brazilian Research Agency CNPq.

6. REFERENCES

Alkmim, M., De Morais, M. and Fabro, A., 2016. "Vibration reduction of wind turbines using tuned liquid column damper using stochastic analysis". In *Journal of physics: conference series*. IOP Publishing, Vol. 744, p. 012178.

Bashkirtseva, I., Ryashko, L. and Ryazanova, T., 2018. "Stochastic sensitivity analysis of the variability of dynamics and transition to chaos in the business cycles model". *Communications in Nonlinear Science and Numerical Simulation*, Vol. 54, pp. 174–184.

De Paula, A.S., Inman, D.J. and Savi, M.A., 2015. "Energy harvesting in a nonlinear piezomagnetoelastic beam subjected to random excitation". *Mechanical Systems and Signal Processing*, Vol. 54, pp. 405–416.

Erturk, A., Hoffmann, J. and Inman, D.J., 2009. "A piezomagnetoelastic structure for broadband vibration energy harvesting". *Applied Physics Letters*, Vol. 94, No. 25, p. 254102.

Feenstra, J., Granstrom, J. and Sodano, H., 2008. "Energy harvesting through a backpack employing a mechanically amplified piezoelectric stack". *Mechanical Systems and Signal Processing*, Vol. 22, No. 3, pp. 721–734.

Lallart, M., Anton, S.R. and Inman, D.J., 2010. "Frequency self-tuning scheme for broadband vibration energy harvesting". *Journal of Intelligent Material Systems and Structures*, Vol. 21, No. 9, pp. 897–906.

Litak, G., Friswell, M.I. and Adhikari, S., 2016. "Regular and chaotic vibration in a piezoelectric energy harvester". *Meccanica*, Vol. 51, No. 5, pp. 1017–1025.

Newland, D.E., 1980. "An introduction to random vibrations and spectral analysis". Technical report, Longman.

Pereira, T.L., de Paula, A.S., Fabro, A.T. and Savi, M.A., 2019. "Random effects in a nonlinear vibration-based piezoelectric energy harvesting system". *International Journal of Bifurcation and Chaos*, Vol. 29, No. 04, p. 1950046.

Rome, L.C., Flynn, L., Goldman, E.M. and Yoo, T.D., 2005. "Generating electricity while walking with loads". *Science*, Vol. 309, No. 5741, pp. 1725–1728.

Sohn, J., Choi, S.B. and Lee, D., 2005. "An investigation on piezoelectric energy harvesting for mems power sources". *Proceedings of the Institution of Mechanical Engineers, Part C: Journal of Mechanical Engineering Science*, Vol. 219, No. 4, pp. 429–436.